From Foundations of Astrophysics
Ryden & Peterson

7 The Sun

Although the Sun is more massive and more luminous than most of the stars in its neighborhood, it is by no means freakishly bright. Thus, by studying the Sun in particular, we can learn a great deal about stars in general. A study of stellar interiors (including the solar interior) will be deferred until Chapter 15, when we will have covered the observable properties of stars in more detail. At this point, however, some discussion of the Sun's outer layers is merited. This is partly because there are aspects of solar physics we need to understand in order to understand the evolution of the solar system as a whole. However, it is also true that the Sun is the only star whose surface has been studied in detail, and thus it deserves some extra attention.

7.1 ▪ OBSERVABLE LAYERS OF THE SUN

An image of the Sun at visible wavelengths (Figure 7.1) has a sharp, well-defined boundary, implying that the Sun has a well-defined surface. The observed surface of the Sun at visible wavelengths is the **photosphere**. More exactly, the photosphere is defined as the layer of the Sun's atmosphere from which nearly all of the observed photons escape. The optical depth τ increases rapidly with depth in the photosphere; as a result, the photosphere is not very thick when compared to the size of the Sun as a whole. The vast majority of the light we observe from the Sun comes from a photosphere only ~ 400 km thick. The base of the photosphere is at a distance $R_\odot = 696{,}000$ km from the Sun's center. It's the thinness of the photosphere that gives the Sun its sharp-edged appearance. The temperature T beneath the photosphere increases with depth, as does the degree of ionization; the interior of the Sun is a hot plasma of free electrons and positively charged ions.

Because the top of the photosphere is cooler than the layers beneath, the photosphere produces absorption lines in the spectrum of the Sun. Detailed analysis of high resolution spectra allows us to deduce the physical properties of the solar photosphere. Elemental abundances, for instance, are very different from those found on Earth. By mass, hydrogen constitutes 73.4% of the photosphere, helium constitutes 25.0%, and

From Foundations of Astrophysics
Ryden & Peterson

FIGURE 7.1 The photosphere is the region of the solar atmosphere from which most of the visible light is emitted. Note the effect of "limb darkening"; the solar disk has a higher surface brightness at the center than at the edges.

all the remaining elements of the periodic table contribute only 1.6% of the mass of the photosphere.[1]

In the photosphere, the principal source of opacity is the **H^- ion**, that is, a hydrogen atom with an additional electron. In a gas containing both neutral hydrogen atoms and free electrons, H^- ions can form by the reaction

$$H + e^- \rightarrow H^- + \gamma. \tag{7.1}$$

Many metals have low ionization potentials and thus are partially ionized at the temperature of the Sun's photosphere; this provides the primary source of free electrons for the creation of H^- ions. However, the second electron in the H^- ion is quite loosely bound, with an ionization energy $\chi = 0.75$ eV. The fragility of the H^- ion implies that it is abundant enough to affect the opacity only under special conditions; the density of gas must be fairly high, and the temperature must be in the range $2500\text{ K} \lesssim T \lesssim 10{,}000\text{ K}$. At lower temperatures, there are essentially no free electrons available, and at higher temperatures, the H^- ions are blasted apart by photons as soon as they form. The energy $\chi = 0.75$ eV required to remove the second electron corresponds to a wavelength $\lambda = 1.7\ \mu$m. This means that when H^- is present, it can absorb ultraviolet photons, visible photons, and infrared photons out to a wavelength of $1.7\ \mu$m. Since the density of particles in the photosphere decreases with height, eventually the density drops to the

[1] Astronomers sometimes lump together all elements heavier than helium as "metals." This puts them, we realize, on the same level as primitive tribes who count "one, two, many," but sometimes the ability to count beyond two is overrated.

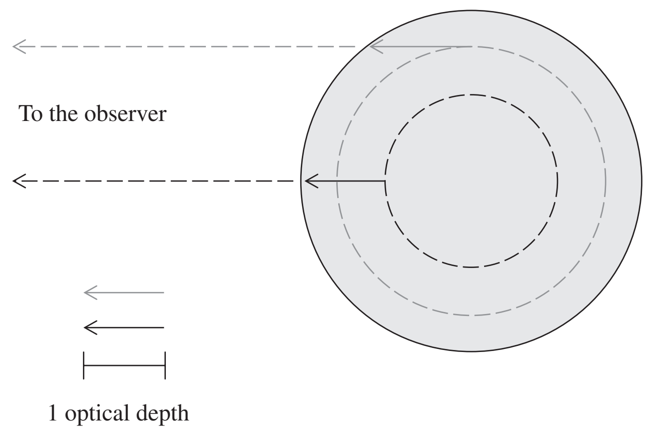

FIGURE 7.2 An observer far to the left observes limb darkening of the Sun. Photons from the center of the Sun's disk come, on average, from deeper, hotter layers of the photosphere.

point where the collisions between free electrons and hydrogen atoms that lead to formation of H^- occur too slowly to keep up with the photodissociation rate. Thus, at the top of the photosphere, the H^- has disappeared, the opacity due to H^- has disappeared, and photons can escape.

The photons that we observe from the photosphere come from a variety of depths, and thus, given the temperature gradient across the photosphere, represent blackbody emission at a range of temperatures. The average depth from which the observed photons originate is determined by the column density of H^- along our line of sight. At the center of the solar disk, the physical depth corresponding to an optical depth $\tau = 1$ is larger than the physical depth at the limb, or edge, of the Sun. This effect is illustrated in Figure 7.2.

As a consequence of this effect, the Sun displays **limb darkening**; the surface brightness is greater at the center of the Sun's disk because the photons we see come from deeper, hotter layers of the photosphere, on average. By comparison, the limb of the Sun's disk is lower in surface brightness because the photons come from higher, cooler layers of the photosphere, on average. The average temperature (that is, the one that gives the best-fitting Planck spectrum) at the center of the disk is $T \approx 6100$ K. However, when photons from the entire disk are pooled together, the best-fitting temperature is $T \approx 5700$ K, thanks to the contribution from the cooler photons from the limb.

When the Sun's disk is viewed at high angular resolution, the photosphere is seen to be broken up into **granules** (Figure 7.3). The granules are convection cells in the photosphere. Hot gas rises at the center of the granule; after the hot gas cools by radiation, the cooler gas sinks back down at the edges of the granules. The typical size of granules is $d \sim 1000$ km, and the typical lifetime of a granule before it breaks up is only $t \sim 10$ minutes. A time-lapse movie of the photosphere looks like a seething vat of soup.

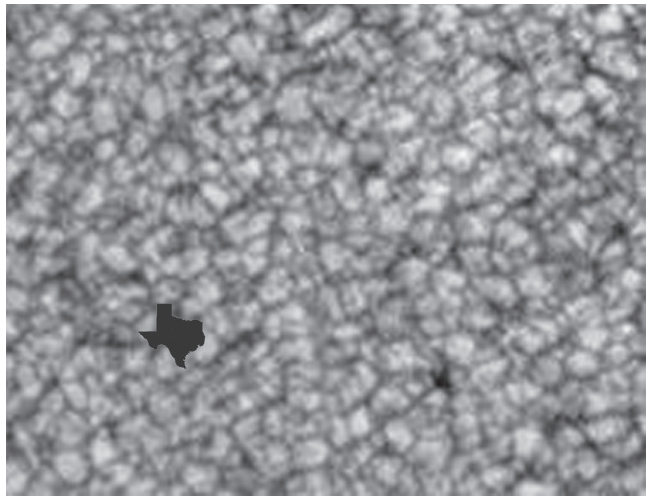

FIGURE 7.3 Detail of the photosphere showing granules; typically, they are the size of Texas ($d \sim 1000$ km).

The **chromosphere** is the layer of the Sun's atmosphere immediately above the photosphere. The chromosphere, as illustrated in Color Figure 4, is most easily seen during a total solar eclipse, when the Moon blocks the light from the much-brighter (by definition) photosphere. The chromosphere produces an emission spectrum, as expected from Kirchhoff's laws; it consists of hot, tenuous gas seen, during an eclipse, against a dark background. The characteristic red color that gives the chromosphere its name[2] is due to strong emission from the Hα λ6563 line. When the emission spectrum of the chromosphere was measured during an eclipse on 1868 August 18, astronomers were surprised to detect a yellow emission line ($\lambda = 5875$ Å) that didn't correspond to any known element. The English scientist Norman Lockyer decided that the line was due to a previously unknown element that he called "helium," after the Sun god Helios. Chemists did not isolate the element helium in their laboratories until 1895, when its emission spectrum was verified.

The temperature of the chromosphere increases with distance from the Sun's center (unlike the temperature structure of the photosphere, where the temperature drops with increasing distance). At the top of the photosphere, which constitutes the base of the chromosphere, the temperature is $T \approx 4400$ K; at the top of the chromosphere, at a height of ~ 2500 km above its base, the temperature has risen sharply to $T \approx 9000$ K.[3]

[2] *Chromo-* is a Greek root meaning "color."

[3] The reason why helium absorption lines are not seen in the Sun's photospheric spectrum is that the cooler temperatures there result in photons that are insufficiently energetic to raise electrons above the ground state of helium.

Recalling the definition of optical depth, Eq. (9.17),

$$\tau_\lambda = \int_0^s \kappa_\lambda \rho \, ds,$$

we see that if the opacity κ_λ increases at some wavelength, then the actual distance back along the ray to the level where $\tau_\lambda = 2/3$ decreases for that wavelength. One cannot see as far into murky material, so an observer will not see as deeply into the star at wavelengths where the opacity is greater than average (i.e., greater than the continuum opacity). This implies that if the temperature of the stellar atmosphere decreases outward, then these higher regions of the atmosphere will be cooler. As a result, the intensity of the radiation at $\tau_\lambda \approx 2/3$ will decline the most for those wavelengths at which the opacity is greatest, resulting in absorption lines in the continuous spectrum. Therefore, the temperature *must* decrease outward for the formation of absorption lines. This is the analog for stellar atmospheres of Kirchhoff's law that a cool, diffuse gas in front of a source of a continuous spectrum produces dark spectral lines in the continuous spectrum.

Limb Darkening

Another implication of receiving radiation from an optical depth of about two-thirds is shown in Fig. 9.12. The line of sight of an observer on Earth viewing the Sun is vertically downward at the center of the Sun's disk but makes an increasingly larger angle θ with the vertical near the edge, or *limb*, of the Sun. Looking near the limb, the observer will not see as deeply into the solar atmosphere and will therefore see a lower temperature at an optical depth of two-thirds (compared to looking at the center of the disk). As a result, the limb of

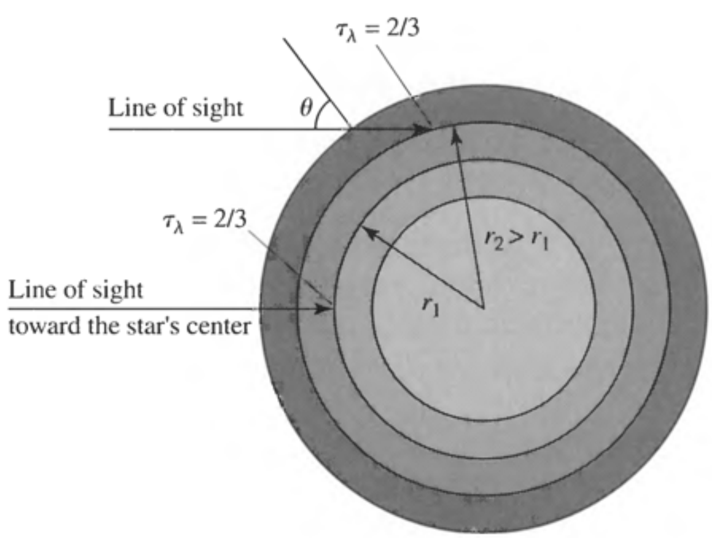

FIGURE 9.12 Limb darkening. The distance traversed within the atmosphere of the star to reach a specified radial distance r from the star's center increases along the line of sight of the observer as θ increases. This implies that to reach a specified optical depth (e.g., $\tau_\lambda = 2/3$), the line of sight terminates at greater distances (and cooler temperatures) from the star's center as θ increases. Note that the physical scale of the photosphere has been greatly exaggerated for illustration purposes. The thickness of a typical photosphere is on the order of 0.1% of the stellar radius.

the Sun appears darker than its center. This **limb darkening** is clearly seen in Fig. 11.11 for the Sun and has also been observed in the light curves of some eclipsing binaries. More detailed information on limb darkening may be found later in this section.

The Radiation Pressure Gradient

Considering the meandering nature of a photon's journey to the surface, it may seem surprising that the energy from the deep interior of the star ever manages to escape into space. At great depth in the interior of the star, the photon's mean free path is only a fraction of a centimeter. After a few scattering encounters, the photon is traveling in a nearly random direction, hundreds of millions of meters from the surface. This situation is analogous to the motions of air molecules in a closed room. An individual molecule moves about with a speed of nearly 500 m s^{-1}, and it collides with other air molecules several billion times per second. As a result, the molecules are moving in random directions. Because there is no overall migration of the molecules in a closed room, a person standing in the room feels no wind. However, opening a window may cause a breeze if a pressure difference is established between one side of the room and the other. The air in the room responds to this pressure gradient, producing a net flux of molecules toward the area of lower pressure.

In a star the same mechanism causes a "breeze" of photons to move toward the surface of the star. Because the temperature in a star decreases outward, the radiation pressure is smaller at greater distances from the center (cf., Eq. 9.11 for the blackbody radiation pressure). This gradient in the radiation pressure produces the slight net movement of photons toward the surface that carries the radiative flux. As we will discover later in this section, this process is described by

$$\frac{dP_{\text{rad}}}{dr} = -\frac{\overline{\kappa}\rho}{c} F_{\text{rad}}. \tag{9.31}$$

Thus the transfer of energy by radiation is a subtle process involving the slow upward diffusion of randomly walking photons, drifting toward the surface in response to minute differences in the radiation pressure. The description of a "beam" or a "ray" of light is only a convenient fiction, used to define the direction of motion momentarily shared by the photons that are continually absorbed and scattered into and out of the beam. Nevertheless, we will continue to use the language of photons traveling in a beam or ray of light, realizing that a specific photon is in the beam for only an instant.

9.4 ■ THE TRANSFER EQUATION

In this section, we will focus on a more thorough examination of the flow of radiation through a stellar atmosphere.[22] We will develop and solve the basic equation of radiative transfer using several standard assumptions. In addition, we will derive the variation of temperature with optical depth in a simple model atmosphere before applying it to obtain a quantitative description of limb darkening.

[22] Although the focus of this discussion is on stellar atmospheres, much of the discussion is applicable to other environments as well, such as light traversing an interstellar gas cloud.

Limb Darkening Revisited

We now move on to take a closer look at limb darkening (recall Fig. 9.12). A comparison of theory and observations of limb darkening can provide valuable information about how the source function varies with depth in a star's atmosphere. To see how this is done, we first solve the general form of the transfer equation (Eq. 9.36),

$$\frac{dI_\lambda}{d\tau_\lambda} = I_\lambda - S_\lambda,$$

at least formally, rather than by making assumptions. (The inevitable assumptions will be required soon enough.) Multiplying both sides by $e^{-\tau_\lambda}$, we have

$$\begin{aligned} \frac{dI_\lambda}{d\tau_\lambda} e^{-\tau_\lambda} - I_\lambda e^{-\tau_\lambda} &= -S_\lambda \, e^{-\tau_\lambda} \\ \frac{d}{d\tau_\lambda}(e^{-\tau_\lambda} I_\lambda) &= -S_\lambda \, e^{-\tau_\lambda} \\ d(e^{-\tau_\lambda} I_\lambda) &= -S_\lambda \, e^{-\tau_\lambda} \, d\tau_\lambda. \end{aligned}$$

If we integrate from the initial position of the ray, at optical depth $\tau_{\lambda,0}$ where $I_\lambda = I_{\lambda,0}$, to the top of the atmosphere, at optical depth $\tau_\lambda = 0$ where $I_\lambda = I_\lambda(0)$, the result for the emergent intensity at the top of the atmosphere, $I_\lambda(0)$, is

$$I_\lambda(0) = I_{\lambda,0} e^{-\tau_{\lambda,0}} - \int_{\tau_{\lambda,0}}^{0} S_\lambda e^{-\tau_\lambda} \, d\tau_\lambda. \tag{9.54}$$

This equation has a very straightforward interpretation. The emergent intensity on the left is the sum of two positive contributions. The first term on the right is the initial intensity of the ray, reduced by the effects of absorption along the path to the surface. The second term, also positive,[28] represents the emission at every point along the path, attenuated by the absorption between the point of emission and the surface.

We now return to the geometry of a plane-parallel atmosphere and the vertical optical depth, τ_v. However, we do *not* assume a gray atmosphere, LTE, or make the Eddington approximation. As shown in Fig. 9.16, the problem of limb darkening amounts to determining the emergent intensity $I_\lambda(0)$ as a function of the angle θ. Equation (9.54), the formal solution to the transfer equation, is easily converted to this situation by using Eq. (9.38) to replace τ_λ with $\tau_{\lambda,v} \sec\theta$ (the vertical optical depth) to get

$$I(0) = I_0 e^{-\tau_{v,0}\sec\theta} - \int_{\tau_{v,0}\sec\theta}^{0} S \sec\theta \, e^{-\tau_v \sec\theta} \, d\tau_v.$$

Although both I and τ_v depend on wavelength, the λ subscript has been dropped to simplify the notation; the approximation of a gray atmosphere has *not* been made. To include the contributions to the emergent intensity from all layers of the atmosphere, we take the value

[28] Remember that the optical depth, measured along the ray's path, decreases in the direction of travel, so $d\tau_\lambda$ is negative.

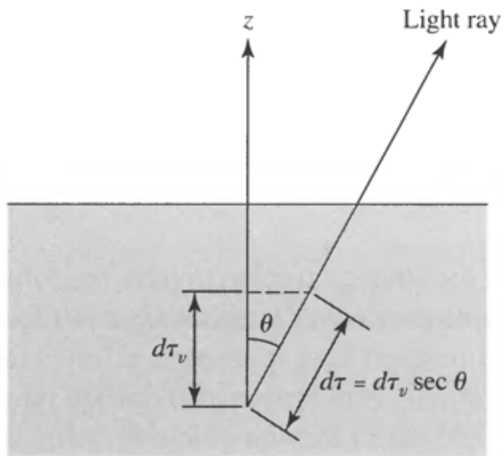

FIGURE 9.16 Finding $I(0)$ as a function of θ for limb darkening in plane-parallel geometry.

of the initial position of the rays to be at $\tau_{v,0} = \infty$. Then the first term on the right-hand side vanishes, leaving

$$I(0) = \int_0^\infty S \sec\theta \, e^{-\tau_v \sec\theta} \, d\tau_v. \tag{9.55}$$

If we knew how the source function depends on the vertical optical depth, this equation could be integrated to find the emergent intensity as a function of the direction of travel, θ, of the ray. Although the form of the source function is not known, a good guess will be enough to estimate $I(0)$. Suppose that the source function has the form

$$S = a + b\tau_v, \tag{9.56}$$

where a and b are wavelength-dependent numbers to be determined. Inserting this into Eq. (9.55) and integrating (the details are left as an exercise) show that the emergent intensity for this source function is

$$I_\lambda(0) = a_\lambda + b_\lambda \cos\theta, \tag{9.57}$$

where the λ subscripts have been restored to the appropriate quantities to emphasize their wavelength dependence. By making careful measurements of the variation in the specific intensity across the disk of the Sun, the values of a_λ and b_λ for the solar source function can be determined for a range of wavelengths. For example, for a wavelength of 501 nm, Böhm-Vitense (1989) supplies values of $a_{501} = 1.04 \times 10^{13}$ W m^{-3} sr^{-1} and $b_{501} = 3.52 \times 10^{13}$ W m^{-3} sr^{-1}.

Example 9.4.2. Solar limb darkening provides an opportunity to test the accuracy of our "plane-parallel gray atmosphere in LTE using the Eddington approximation." In the preceding discussion of an equilibrium gray atmosphere, it was found that the mean intensity is equal to the source function,

$$\langle I \rangle = S$$

continued

(Eq. 9.44). Then, with the additional assumptions of the Eddington approximation and LTE, Eqs. (9.52) and (9.53) can be used to determine the mean intensity and thus the source function:

$$S = \langle I \rangle = \frac{\sigma T^4}{\pi} = \frac{3\sigma}{4\pi} T_e^4 \left(\tau_v + \frac{2}{3} \right).$$

Taking the source function to have the form of Eq. (9.56), $S = a + b\tau_v$, as used earlier for limb darkening (*after integrating over all wavelengths*), the values of the coefficients are

$$a = \frac{\sigma}{2\pi} T_e^4 \qquad \text{and} \qquad b = \frac{3\sigma}{4\pi} T_e^4.$$

The emergent intensity then will have the form of Eq. (9.57), $I(0) = a + b\cos\theta$ (again after integrating over all wavelengths). The ratio of the emergent intensity at angle θ, $I(\theta)$, to that at the center of the star, $I(\theta = 0)$, is thus

$$\frac{I(\theta)}{I(\theta = 0)} = \frac{a + b\cos\theta}{a + b} = \frac{2}{5} + \frac{3}{5}\cos\theta. \tag{9.58}$$

We can compare the results of this calculation with observations of solar limb darkening in integrated light (made by summing over all wavelengths). Figure 9.17 shows both the observed values of $I(\theta)/I(\theta = 0)$ and the values from Eq. (9.58). The agreement is remarkably good, despite our numerous approximations. However, be forewarned that the agreement is much worse for observations made at a given wavelength (see Böhm-Vitense, 1989) as a consequence of wavelength-dependent opacity effects such as line blanketing.

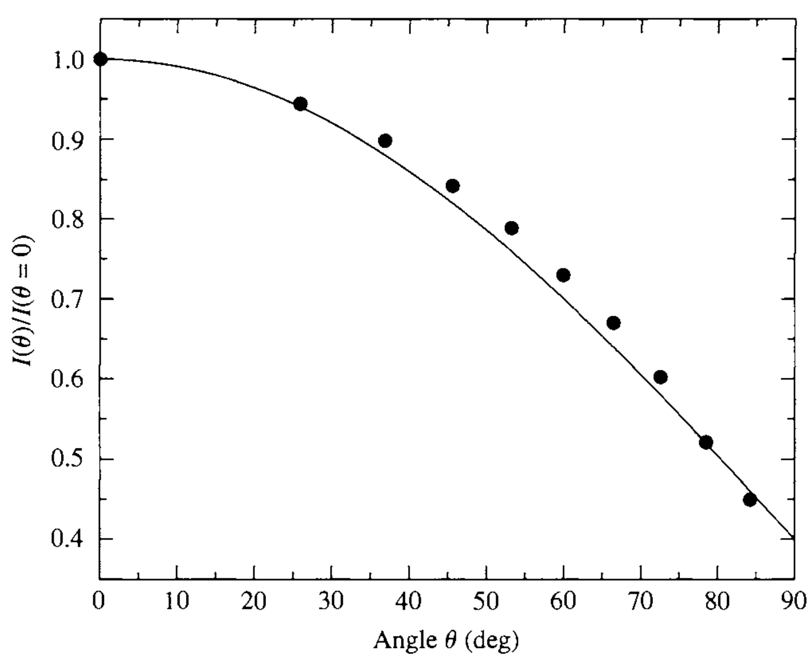

FIGURE 9.17 A theoretical Eddington approximation of solar limb darkening for light integrated over all wavelengths. The dots are observational data for the Sun. Although a good fit, the Eddington approximation is not perfect, which implies that a more detailed model must be developed; see, for example, Problem 9.29.